Three-Dimensional Pulse-Width Modulation Technique in Three-Level Power Inverters for Three-Phase Four-Wired System

Man-Chung Wong, *Student Member, IEEE*, Zheng-Yi Zhao, Ying-Duo Han, *Senior Member, IEEE*, and Liang-Bing Zhao

***Abstract*—Shunt-connected trilevel power inverter in three-phase four-wired system as an active filter or individual current supply (peak-load supply) is studied by a novel technique: Three-dimensional (3-D) voltage vectors pulse width modulation (PWM). In past decades, almost all the study for PWM is limited in two-dimensional (2-D) domain, α and β frames, in three-phase three-wired system. However, in practical operation, there are many three-phase four-wired systems in distribution sites. The generalized study of 3-D two-level and three-level inverters is achieved in this paper so as to perform the basic theory of 3-D multilevel space vector switching PWM technique. The sign cubical hysteresis control strategy is proposed and studied with simulation results in 3-D aspect. The 3-D PWM technique in three-level inverters is accomplished.**

***Index Terms*—Multilevel inverter, power quality, three-dimensional PWM, three-phase four-wired system.**

I. Introduction

FOR THE high voltage power applications where no semiconductor devices are available, the multilevel VSI topologies [7], [8] are good alternatives. The multilevel structure not only reduces voltage stress across the switches but also has many more available vectors. Therefore, it improves harmonic contents of the VSI by selecting appropriate switching vectors. The most popular topology is the three-level inverter [10]. The number of vectors, which can be implemented with the three-level VSI, is 27. These can be categorized into four different vectors: large-vectors, mid-vectors, small-vectors, and zero-vectors.

In recent decades, there are many papers discussing three-phase three-wired systems in the application of active filters or motor-drivers. However, there are seldom papers to take the consideration of three-phase four-wired systems [1]–[4]. Actually, the three-phase four-wired system is also an important part of the power networks. Conventionally, four arms-inverter [9] (Fig. 1) is employed to handle three-phase four-wire power quality problems such as an active filter in abc frames and zero frame. One arm of the inverter is dedicated for compensation of zero component issue. In this study, the focus will be taken for three-phase four-wired systems in the switching manner for three-dimensional (3-D) pulse width modulation (PWM) technique. The two-dimensional (2-D) PWM technique will be extended into 3-D one, meanwhile three-level switching patterns are studied. The mathematical model of the trilevel shunt converter is addressed in detail. Based on the concept of switching function and space vector, the mathematical model of trilevel converter model is presented. A novel prototype of three-level converters is studied. The PWM of three-phase four-wired three-level converters will give more degree of freedom for the switching patterns so that 3-D space vector pulse width modulation (3-D-SVPWM) will be addressed. A novel analysis of 3-D three-level inverters is achieved and the generalized theory of 3-D PWM including the 2-D two-level one is studied and developed such that 2-D two-level converters is a subset of the 3-D one. A new approach control method is performed and called "Sign Cubical Hysteresis Control Strategy" in three-phase four-wired systems. Simulation of three-level three-phase four-wired system as an individual current supply and an active filter are also achieved. Practical consideration and comparison with two-level 3-D inverter are performed.

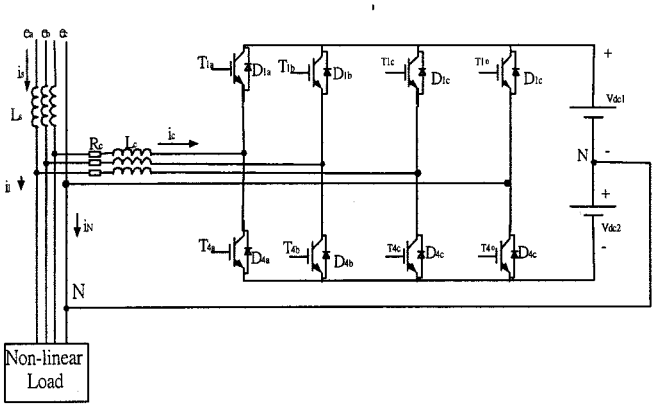

Fig. 1. Conventional strategy to handle three-phase four-wires problem—four arms-inverter.

II. Trilevel Converter and its Mathematical Model

The structure of voltage source shunt trilevel converter is shown as the power quality compensator, motor drivers or peak-load power supply in Fig. 2. The basic principle is to inject the

Manuscript received April 10, 2000; revised January 1, 2001. This work was supported by the Ph.D. Fund, Chinese Education Ministry and Research Fund, University of Macau. Recommended by Associate Editor F. Z. Peng.

M.-C. Wong and Y.-D. Han are with the Faculty of Science and Technology, University of Macau, Macau, China (e-mail: fstmcw@umac.mo).

Z.-Y. Zhao and L.-B. Zhao are with the Department of Electrical Engineering, Tsinghua University, Beijing, China.

Publisher Item Identifier S 0885-8993(01)04034-0.

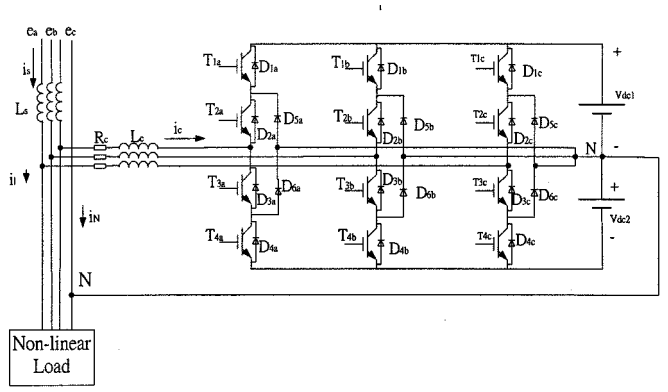

Fig. 2. Hardware of trilevel power inverter in three-phase four-wired system.

same negative amplitude of harmonics into the load current in order to compensate the harmonic current and the in-phase current into the system to reduce the peak-load power supply from the generator [5], [6]. The losses of the switching devices and snubber circuits, and process of commutation are ignored so that the equivalent switched-circuit can be obtained as Fig. 3.

The model of shunt three-phase four-wire three-level converter is investigated in the a-b-c frame. Switching functions can be considered as the equivalent switched devices such as IGBT's, e.g., in phase A, S_a may be written as

$$S_a = \begin{cases} 1, & \text{when } T_{1a} \text{ and } T_{2a} \text{ are closed } (S_{1a}) \\ 0, & \text{when } T_{2a} \text{ and } T_{3a} \text{ are closed } (S_{3a}) \\ -1, & \text{when } T_{3a} \text{ and } T_{4a} \text{ are closed } (S_{2a}). \end{cases} \tag{1}$$

There are three cases in one arm of the three-level converters such as positive, zero or negative switching function

1) if $S_a = 1$, then $S_{1a} = 1,\ S_{2a} = 0,\ S_{3a} = 0$
2) if $S_a = 0$, then $S_{1a} = 0,\ S_{2a} = 0,\ S_{3a} = 1$
3) if $S_a = -1$, then $S_{1a} = 0,\ S_{2a} = 1,\ S_{3a} = 0$.

It is noticed that S_a, S_b and S_c can be 1, 0 and -1. In the Fig. 3, the boundary condition of S_{1a}, S_{2a} and S_{3a} is defined as

$$\begin{cases} S_{1a} + S_{2a} + S_{3a} = 1 \\ S_{1a} = 1 \text{ or } 0, \quad S_{2a} = 1 \text{ or } 0, \quad S_{3a} = 1 \text{ or } 0. \end{cases} \tag{2}$$

It means that when S_{1a} is equal to 1 then S_{2a} and S_{3a} must be zero. The relation among the ac-side compensating current, the terminal voltage of the inverter can be expressed as equation (3) according to Fig. 3

$$\begin{cases} L_c \dfrac{di_{ca}}{dt} = -R_c \cdot i_{ca} - v_a + v_{sa} \\ L_c \dfrac{di_{cb}}{dt} = -R_c \cdot i_{cb} - v_b + v_{sb} \\ L_c \dfrac{di_{cc}}{dt} = -R_c \cdot i_{cc} - v_c + v_{sc}. \end{cases} \tag{3}$$

By using the switching functions, the relation between the terminal voltage (v_a, v_b, v_c) and the dc-link voltage (v_{dc1}, v_{dc2}) can be expressed as (4)

$$\begin{cases} v_a = S_{1a} \cdot v_{\mathrm{dc1}} - S_{2a} \cdot v_{\mathrm{dc2}} \\ v_b = S_{1b} \cdot v_{\mathrm{dc1}} - S_{2b} \cdot v_{\mathrm{dc2}} \\ v_c = S_{1c} \cdot v_{\mathrm{dc1}} - S_{2c} \cdot v_{\mathrm{dc2}}. \end{cases} \tag{4}$$

A general mathematical model of the trilevel Converter in three-phase four-wire system can be established as follows:

$$\boldsymbol{Z}\dot{\boldsymbol{X}} = \boldsymbol{A}\boldsymbol{X} + \boldsymbol{B}\boldsymbol{U} \tag{5}$$

where

$$\mathbf{A} = \begin{bmatrix} -R_c & 0 & 0 & -S_{1a} & S_{2a} \\ 0 & -R_c & 0 & -S_{1b} & S_{2b} \\ 0 & 0 & -R_c & -S_{1c} & S_{2c} \end{bmatrix}$$

$$\boldsymbol{X} = [\, i_{ca} \quad i_{cb} \quad i_{cc} \quad V_{\mathrm{dc1}} \quad V_{\mathrm{dc2}} \,]^T$$

$$\mathbf{B} = \mathrm{diag}\,[1 \quad 1 \quad 1]$$

$$\mathbf{U} = [\, v_{sa} \quad v_{sb} \quad v_{sc} \,]$$

$$\mathbf{Z} = \mathrm{diag}\,[L_c \quad L_c \quad L_c].$$

III. Two-Level and Three-Level Three-Dimensional Voltage Vectors in Three-Phase Four-Wired System

In three-phase three-wire systems, two-dimensional (2-D) vector control is utilized. Only 2-D control method cannot be used to compensate all the issues in three-phase four-wire systems due to the presence of neutral current (zero-sequence component). This section presents equations that relate to three-dimensional (3-D) vector control not only for the two-level converter but also for the three-level one. This proposed technique could be used to control the three-level VSI as an active filter for power quality improvement.

The instantaneous voltage in α–β–0 frame can be transferred from a–b–c frame by the matrix $[P]$, such as shown in (6)

$$\begin{bmatrix} v_\alpha \\ v_\beta \\ v_0 \end{bmatrix} = [P] \begin{bmatrix} v_a \\ v_b \\ v_c \end{bmatrix} \tag{6}$$

where

$$[P] = \sqrt{\frac{2}{3}} \begin{bmatrix} 1 & -1/2 & -1/2 \\ 0 & \sqrt{3}/2 & -\sqrt{3}/2 \\ 1/\sqrt{2} & 1/\sqrt{2} & 1/\sqrt{2} \end{bmatrix}.$$

The instantaneous voltage vector can be expressed as (7)

$$\vec{V}_S = \sqrt{\frac{2}{3}} \left(V_{SA} + \alpha \cdot V_{SB} + \alpha^2 \cdot V_{SC} \right) \tag{7}$$

where

$$\alpha = e^{j(2\pi/3)}, \qquad \alpha^2 = e^{-j(2\pi/3)}.$$

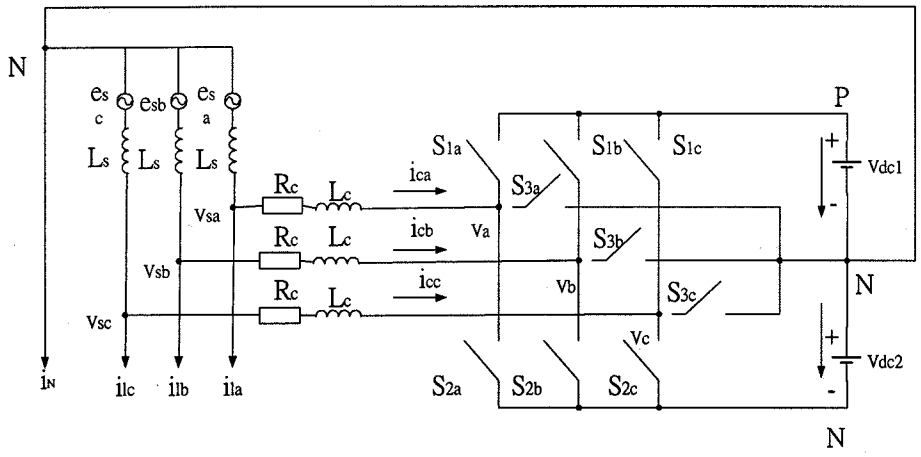

Fig. 3. Equivalent model of trilevel inverters.

According to the switching functions defined in (1), (7) can be expressed in α–β–0 frame as shown in (8). It is assumed that $V_{\rm dc1} = V_{\rm dc2} = V_{\rm dc}$

$$V_s = V_{\rm dc}\left[i\sqrt{\frac{2}{3}}\left(S_a - \frac{1}{2}\cdot S_b - \frac{1}{2}\cdot S_c\right) + j\frac{1}{\sqrt{2}}(S_b - S_c) + k\left(\frac{1}{\sqrt{3}}(S_a + S_b + S_c)\right)\right]. \quad (8)$$

Furthermore, (8) can be redefined as (9)

$$V_s = V_{\rm dc}\left[i\sqrt{\frac{2}{3}}S_\alpha + j\frac{1}{\sqrt{2}}S_\beta + k\frac{1}{\sqrt{3}}S_0\right] \quad (9)$$

where

$$S_\alpha = S_a - \tfrac{1}{2}S_b - \tfrac{1}{2}S_c$$
$$S_\beta = S_b - S_c$$
$$S_0 = S_a + S_b + S_c.$$

Figs. 4 and 5 show the conventional Space Vector Allocation for two-level and three-level converters respectively. According to (9), there are four tables expressing the large-voltage, medium-voltage, small-voltage, and zero-voltage space vector allocation in α–β–0 frame, respectively, for three level converters. If the network has accessible neutral wire, a zero-sequence current component can exit. It is desired that the load current zero-sequence component be compensated by the active power filter or by the unbalance current compensator. For these cases, the zero-sequence converter current component, as well as the other components, must be controlled. The voltage vectors in Tables I–IV can be referred in Fig. 5 to express the actual location in α-β frame. Fig. 6 shows the voltage space vector in S_α–S_β–S_0 frame, for example, $\vec{V}_{2(+++)}$ means that the location of this vector will be in first quadrant in α and β axes with positive value in 0-axis. It was shown in Figs. 7 and 8, which have vectors: $\vec{V}_{2(+++)}$, $\vec{V}_{01n(+0-)}$ and $\vec{V}_{6(+-+)}$. Actually, all vectors in three-level or two-level voltage source inverters will be located in 3-D aspects for three-phase four-wired system. When we further have consideration between two-level

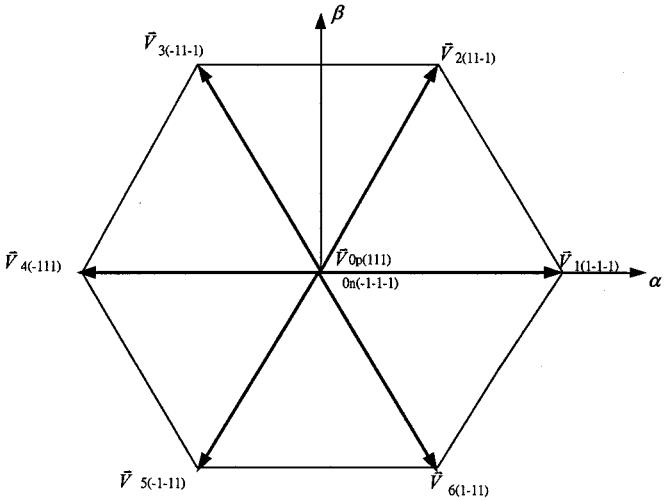

Fig. 4. Two-level voltage vectors allocation.

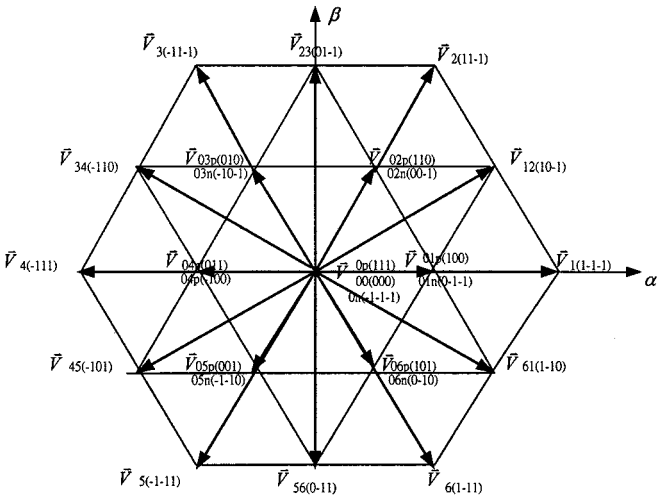

Fig. 5. Three-level voltage vectors allocation.

3-D and three-level 3-D systems, it can be found that actually in two-level system, what we have are the vectors in Tables I and IV only. It will be obvious to conclude that a set of

TABLE I
LARGE VECTORS

	S_a	S_b	S_c	S_α	S_β	S_0
$\vec{V}_1$	1	-1	-1	2	0	-1
$\vec{V}_2$	1	1	-1	1	2	1
$\vec{V}_3$	-1	1	-1	-1	2	-1
$\vec{V}_4$	-1	1	1	-2	0	1
$\vec{V}_5$	-1	-1	1	-1	-2	-1
$\vec{V}_6$	1	-1	1	1	-2	1

TABLE II
MEDIUM VECTORS

	S_a	S_b	S_c	S_α	S_β	S_0
$\vec{V}_{12}$	1	0	-1	1.5	1	0
$\vec{V}_{23}$	0	1	-1	0	2	0
$\vec{V}_{34}$	-1	1	0	-1.5	1	0
$\vec{V}_{45}$	-1	0	1	-1.5	-1	0
$\vec{V}_{56}$	0	-1	1	0	-2	0
$\vec{V}_{61}$	1	-1	0	1.5	-1	0

TABLE III
SMALL VECTORS

	S_a	S_b	S_c	S_α	S_β	S_0
$\vec{V}_{01p}$	1	0	0	1	0	1
$\vec{V}_{01n}$	0	-1	-1	1	0	-2
$\vec{V}_{02p}$	1	1	0	0.5	1	2
$\vec{V}_{02n}$	0	0	-1	0.5	1	-1
$\vec{V}_{03p}$	0	1	0	-0.5	1	1
$\vec{V}_{03n}$	-1	0	-1	-0.5	1	-2
$\vec{V}_{04p}$	0	1	1	-1	0	2
$\vec{V}_{04n}$	-1	0	0	-1	0	-1
$\vec{V}_{05p}$	0	0	1	-0.5	-1	1
$\vec{V}_{05n}$	-1	-1	0	-0.5	-1	-2
$\vec{V}_{06p}$	1	0	1	0.5	-1	2
$\vec{V}_{06n}$	0	-1	0	0.5	-1	-1

TABLE IV
ZERO VECTORS

	S_a	S_b	S_c	S_α	S_β	S_0
$\vec{V}_{000}$	0	0	0	0	0	0
$\vec{V}_{00p}$	1	1	1	0	0	3
$\vec{V}_{00n}$	-1	-1	-1	0	0	-3

two-level 3-D voltage space vectors is a subset of three-level 3-D system. Comparing two-level and three-level inverters for power quality compensator in 3-D PWM technique, however, it will be found that three-level inverter can give more better performance than in two-level 3-D PWM technique by the same control manner with the same switching frequency. In additional to that, three-level inverter can be applied in higher power application. The reason will be explained in the following sections, especially in Section V.

IV. SIGN CUBICAL (OR RECTANGULAR BAR) HYSTERESIS CURRENT CONTROLLER

A. Basic Control Strategy

In this section, the control strategy for three-level 3-D voltage inverter in three-phase four-wire system is described by

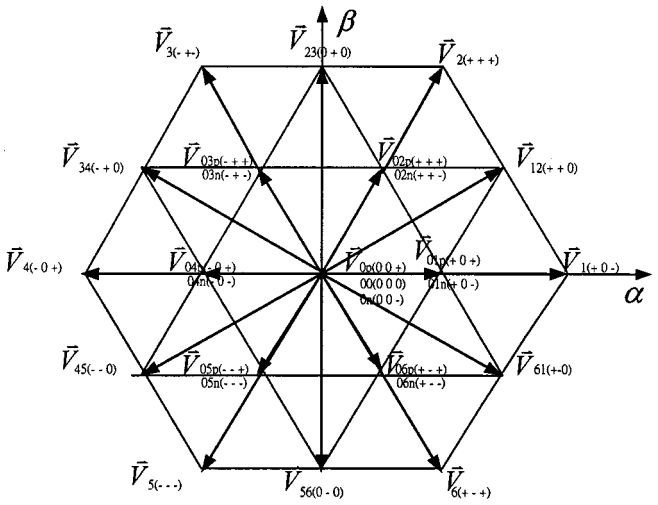

Fig. 6. Three-level voltage vectors allocation in S_α–S_β–S_0 frame.

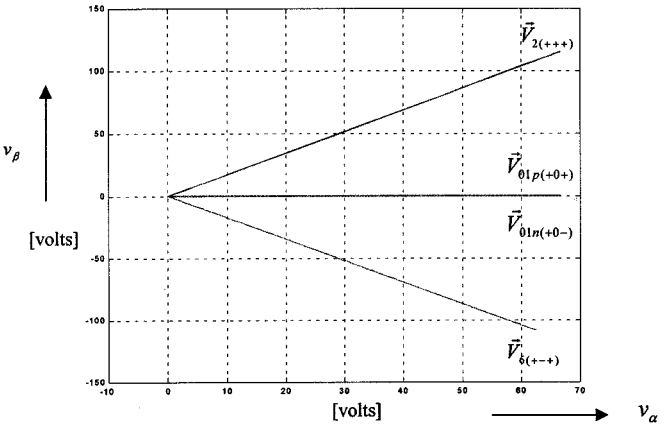

Fig. 7. Two-dimensional vectors in α–β frame.

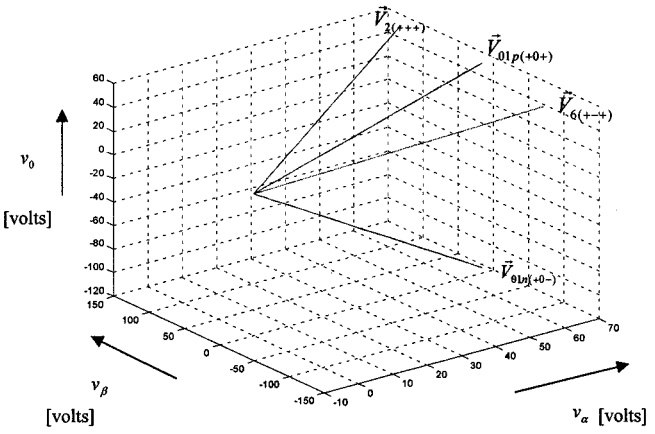

Fig. 8. Vectors in 3-D: α–β–0 frame.

sign cubical hysteresis current controller or sign rectangular bar hysteresis current controller. The basic concept of this control strategy is explained in Fig. 9. The hysteresis limits of $\Delta\alpha$, $\Delta\beta$ and $\Delta 0$ can be equal to each other ($\Delta\alpha = \Delta\beta = \Delta 0$) so as to have cubical control technique, however, they may not equal to each other so that rectangular bar control hysteresis strategy

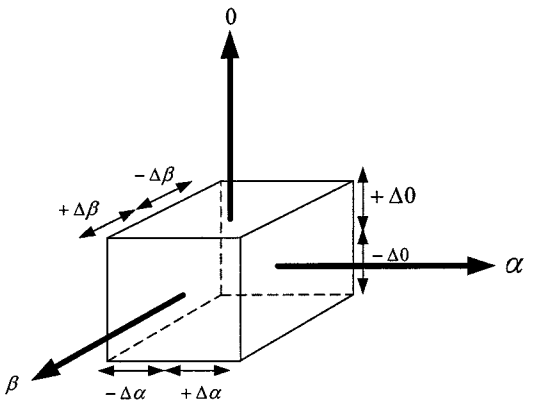

Fig. 9. Concept of sign cubical hysteresis control strategy.

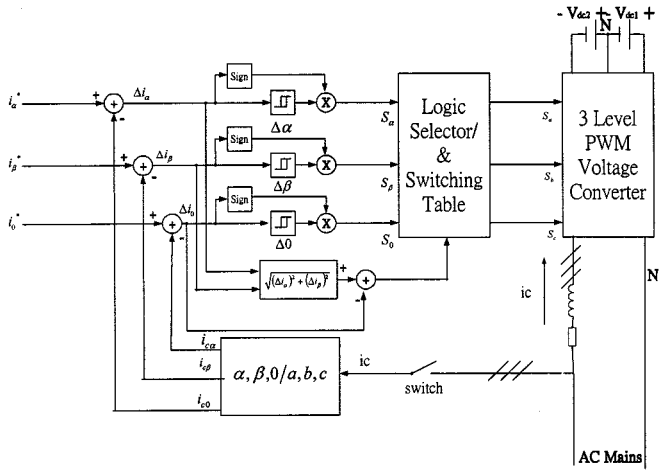

Fig. 10. Control strategy.

is employed. There are three voltage levels $\{1, 0, -1\}$ in three-level voltage inverter so that the sign of triggering pulses is an important parameter in tracking the current reference so as to choose the correct vectors. When the difference between the reference signal and actual input signal is larger than the hysteresis limited value, it will trigger to positive or, vice versa, to negative one. However, when the difference is less than the hysteresis limit, there will be the zero level. In Fig. 10, the injected current of the trilevel converter is detected and transferred from a–b–c frame into α–β–0 frame. The difference between the current reference and the actual load current would be the signal to compare with the injected current signal

$$i^*_{\alpha\beta 0} = i^{reference}_{\alpha\beta 0} - i^{load}_{\alpha\beta 0} \tag{10}$$

$i^{reference}_{\alpha\beta 0}$ is the reference signal that can be obtained by instantaneous reactive power compensation technique, $i^{load}_{\alpha\beta 0}$ is the actual load current that may be distorted by nonlinear load, and the difference between the reference signal and load current signal will be the tracking current ($i^*_{\alpha\beta 0}$) that should be injected by the inverter

$$\Delta i_{\alpha\beta 0} = i^*_{\alpha\beta 0} - i_{c\alpha\beta 0}. \tag{11}$$

The difference between the tracking current ($i^*_{\alpha\beta 0}$) and the coupling current ($i_{c\alpha\beta 0}$) between the inverter and the load terminal will be the control signal ($\Delta i_{\alpha\beta 0}$) to the controller to control the action of inverter.

TABLE V
VECTORS-PAIR

	S_α	S_β	S_0	Large Vectors	Small Vectors
1	+	0	-	$\vec{V}_1$	$\vec{V}_{01\,n}$
2	+	+	+	$\vec{V}_2$	$\vec{V}_{02\,p}$
3	-	+	-	$\vec{V}_3$	$\vec{V}_{03\,n}$
4	-	0	+	$\vec{V}_4$	$\vec{V}_{04\,p}$
5	-	-	-	$\vec{V}_5$	$\vec{V}_{05\,n}$
6	+	-	+	$\vec{V}_6$	$\vec{V}_{06\,p}$

TABLE VI
AMPLITUDE COMPARISON OF VECTORS-PAIR

	$V_{\alpha\beta}$	V_0
$\vec{V}_1, \vec{V}_2, \vec{V}_3, \vec{V}_4, \vec{V}_5, \vec{V}_6$	1.633	0.577
$\vec{V}_{01\,n}, \vec{V}_{02\,p}, \vec{V}_{03\,n}, \vec{V}_{04\,p}, \vec{V}_{05\,n}, \vec{V}_{06\,p}$	0.816	1.154

B. Switching Table and Selection

1) Vector-Pairs: The Hysteresis limit is a solid cube or rectangular bar in 3-D aspect for α–β–0 frame. When all the $\Delta i_{\alpha\beta 0}$ signals are larger than the Hysteresis limit in positive direction so that $S_{\alpha\beta 0} = [+\,+\,+]$. However, if we further consider the Table I (Larger Vectors) and Table III (Small Vectors). It is obvious that this sign cubical or rectangular bar hysteresis Control method will have two vectors in same manner (direction) such as $\vec{V}_1$ and $\vec{V}_{01n}$, $\vec{V}_2$ and $\vec{V}_{02p}$, $\vec{V}_3$ and $\vec{V}_{03n}$, $\vec{V}_4$ and $\vec{V}_{04p}$, $\vec{V}_5$ and $\vec{V}_{05n}$, and, $\vec{V}_6$ and $\vec{V}_{06p}$. For example, $\vec{V}_5$ and $\vec{V}_{05n}$, both vectors will occur at $S_\alpha < 0$, $S_\beta < 0$ and $S_0 < 0$. Table V shows those vector-pairs. There are six pair-vectors with the same directions respectively but with different amplitudes in $v_{\alpha\beta}$ and v_0

$$|V_s| = V_{\rm dc}\left[\sqrt{\left(\sqrt{\frac{2}{3}}\,S_\alpha\right)^2 + \left(\frac{1}{\sqrt{2}}\,S_\beta\right)^2} + \left(\frac{1}{\sqrt{3}}\,S_0\right)^2\right]$$
$$= V_{\rm dc}\left[V^2_{\alpha\beta} + V^2_0\right] \tag{12}$$

where

$$V_{\alpha\beta} = \sqrt{\left(\sqrt{\frac{2}{3}}\,S_\alpha\right)^2 + \left(\frac{1}{\sqrt{2}}\,S_\beta\right)^2}$$

$$V_0 = \frac{1}{\sqrt{3}}\,S_0.$$

According to the (12), the amplitude comparison of vector-pair is achieved in Table VI. It shows that the large vector-pair will pay more action in α–β frame, but it gives less action in zero direction than small vector-pair. For example, $S_\alpha = -1$, $S_\beta = -2$ and $S_0 - 1$ for $\vec{V}_5$, but $S_\alpha = -0.5$, $S_\beta = -1$ and $S_0 - 2$ for $\vec{V}_{05n}$ in this case, $\vec{V}_{05n}$ will take more action than $\vec{V}_5$ in zero sequence compensation. At any time, one vector has to be chosen from these pair-vectors. The error amplitude of $\sqrt{(\Delta i_\alpha)^2 + (\Delta i_\beta)^2}$ is compared with Δi_0, the largest one will

TABLE VII
SPECIAL VECTORS

	S_α	S_β	S_0	Possible Selection Vectors			
1	+	0	0	$\vec{V}_1$	$\vec{V}_{12}$	$\vec{V}_{01\,p}$	$\vec{V}_{01\,n}$
2	-	0	0	$\vec{V}_4$	$\vec{V}_{45}$	$\vec{V}_{04\,p}$	$\vec{V}_{04\,n}$
3	0	+	+	$\vec{V}_{23}$	$\vec{V}_{00\,p}$	$\vec{V}_{02\,p}$	$\vec{V}_{03\,p}$
4	0	+	-	$\vec{V}_{23}$	$\vec{V}_{00\,n}$	$\vec{V}_{02\,n}$	$\vec{V}_{03\,n}$
5	0	-	-	$\vec{V}_{56}$	$\vec{V}_{00\,n}$	$\vec{V}_{06\,n}$	$\vec{V}_{05\,n}$
6	0	-	+	$\vec{V}_{56}$	$\vec{V}_{00\,p}$	$\vec{V}_{06\,p}$	$\vec{V}_{05\,p}$

TABLE VIII
FINAL TABLE

	S_α S_β S_0	S_a S_b S_c		S_α S_β S_0	S_a S_b S_c	S_a S_b S_c
1	+ + -	0 0 -1	15	0 0 0	0 0 0	
2	+ - -	0 -1 0	16	+ 0 0	1 -1 -1	
3	- + +	0 1 0	17	- 0 0	-1 1 1	
4	- - +	0 0 1	18	0 + +	0 1 -1	
5	+ + 0	1 0 -1	19	0 + -	0 1 -1	
6	+ - 0	1 -1 0	20	0 - -	0 -1 1	
7	- + 0	-1 1 0	21	0 - +	0 -1 1	
8	- - 0	-1 0 1			Larger $V_{\alpha\beta}$	Larger V_0
9	0 + 0	0 1 -1	22	+ + +	1 1 -1	1 1 0
10	0 - 0	0 -1 1	23	+ - +	1 -1 1	1 0 1
11	+ 0 +	1 0 0	24	- + -	-1 1 -1	-1 0 -1
12	- 0 -	-1 0 0	25	- - -	-1 -1 1	-1 -1 0
13	0 0 +	1 1 1	26	+ 0 -	1 -1 -1	0 -1 -1
14	0 0 -	-1 -1 -1	27	- 0 +	-1 1 1	0 1 1

be chosen so that it can be decided to activate which vector from those pair-vectors to reduce error. Finally, Fig. 10 will be the control strategy for three-level 3-D voltage inverter in three-phase four-wire system.

2) Special Vectors: According to the above described control strategy, all the vectors can be uniquely defined except the listed six directions in Table VII. In Table VII, for example, there are many selections for compensation, four possible selective vectors are listed only. When the controller received the signals, e.g., $S_\alpha > 0$, $S_\beta = 0$ and $S_0 = 0$, the vector can be selected from $\vec{V}_1$, $\vec{V}_{12}$, $\vec{V}_{01p}$ or $\vec{V}_{01n}$. However, it is because $\vec{V}_1 = \{S_\alpha, S_\beta, S_0\} = [2, 0, -1]$ from Table I, $\vec{V}_{12} = \{S_\alpha, S_\beta, S_0\} = [1.5, 1, 0]$ from Table II, $\vec{V}_{01p} = \{S_\alpha, S_\beta, S_0\} = [1, 0, 1]$ from Table III and $\vec{V}_{01n} = \{S_\alpha, S_\beta, S_0\} = [1, 0, -2]$ from Table III. It can be obvious that those vectors ($\vec{V}_1$, $\vec{V}_{12}$, $\vec{V}_{01p}$ or $\vec{V}_{01n}$) can give different action in α frame, β frame and 0 frame respectively. The vectors $\vec{V}_{01p}$ and $\vec{V}_{01n}$ will give improvement in α frame, but they will force the increase of zero axis error in positive and negative direction respectively. The vector $\vec{V}_{12}$ can give greater enhancement in α frame, but it will increase the error in β frame. On the other hand, $\vec{V}_1$ will provide highest improvement in α frame but with the dedication of zero sequence error. Based on the above discussion, $\vec{V}_1$ should be selected among those vectors so as to choose the first column of possible selected vectors in Table VII.

3) Final Table: There are totally 27 possible combinations in three-level converter. Table VIII will show the final logic-switching table of the control strategy in Fig. 10. The sign of the $S_\alpha\, S_\beta\, S_0$ are the important parameter to determine the voltage vector. When the sign is positive or negative, it means that the signal is larger than the hysteresis limit. When it is zero, the error signal is within the hysteresis limit. According to the Table VIII and logic selection, the switching command can be determined uniquely.

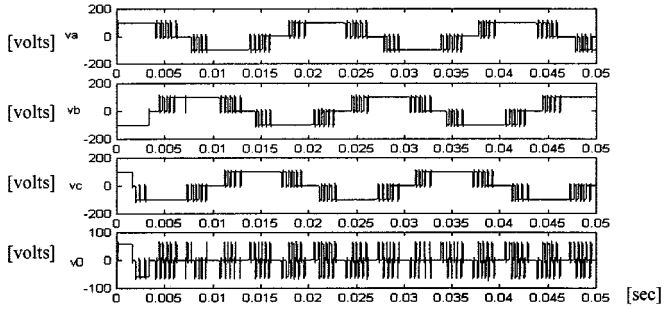

Fig. 11. Three-level voltage waveforms.

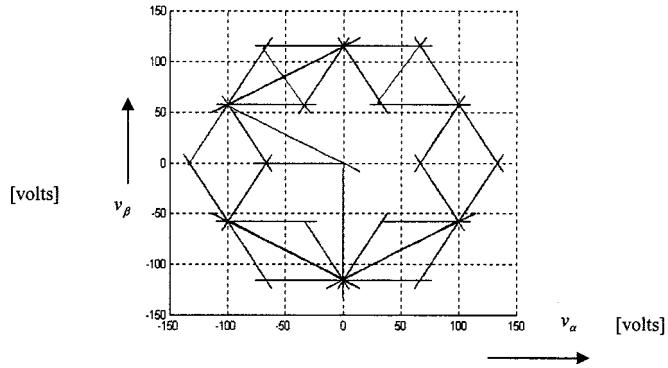

Fig. 12. Voltage vectors in 2-D.

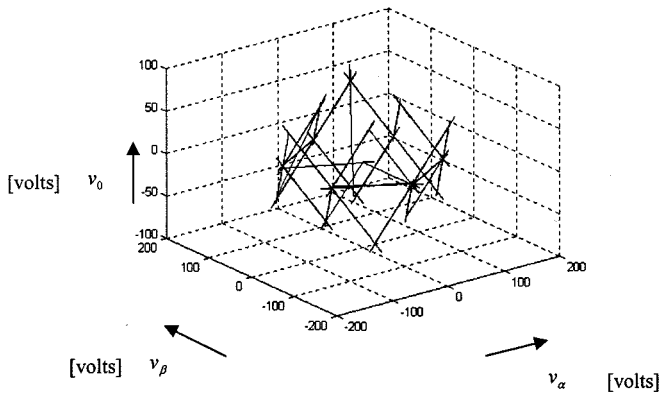

Fig. 13. Voltage vectors in 3-D.

V. SIMULATION RESULTS AND DISCUSSION

The simulation is performed by MATLAB as the individual current supply unit and power quality compensator with random switching frequency and fixed maximum switching frequency.

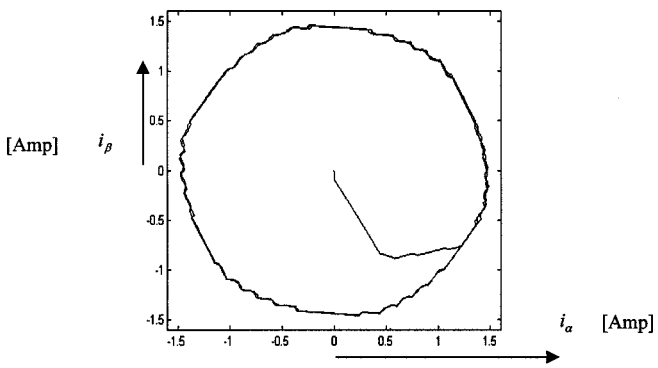

Fig. 14. Current locus in α–β frame.

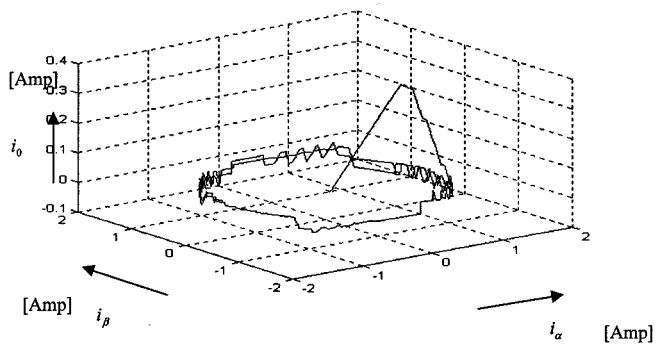

Fig. 15. Current locus in α–β–0 frame.

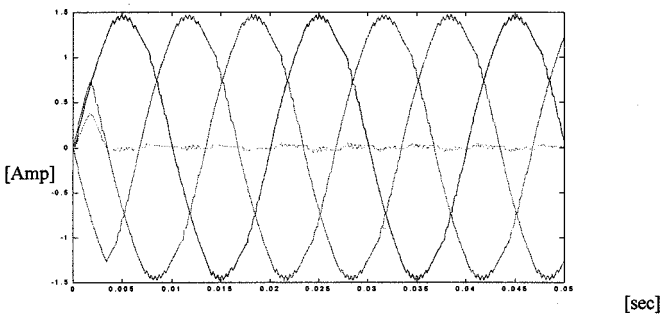

Fig. 16. Current waveforms in individual current supply application.

A. Individual Current Supply Unit

The simulation results as the individual current supply unit are shown in Figs. 11–16. A R-L load is connected to this three-level three-phase four-wire inverter to test its performance. Fig. 11 is the voltage waveforms in phase a, phase b, phase c and neutral line. The voltage space vectors locus is shown in Fig. 12 in 2-D aspect. However, 3-D aspect of Voltage vectors is shown in Fig. 13. The current orbits in α–β frame, in α–β–0 frame and time domain are shown in Figs. 14–16, respectively.

B. Active Filter with Random Switching Frequency

Another simulation is performed as an active filter for nonlinear load and the results are shown in Figs. 17–21. The switch in Fig. 10 (control strategy) is always closed in this case. Fig. 17 shows the current waveforms before compensation. Fig. 18

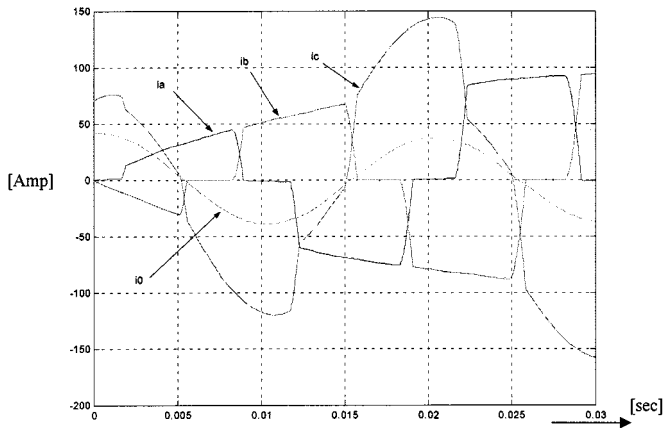

Fig. 17. Current waveforms before compensation.

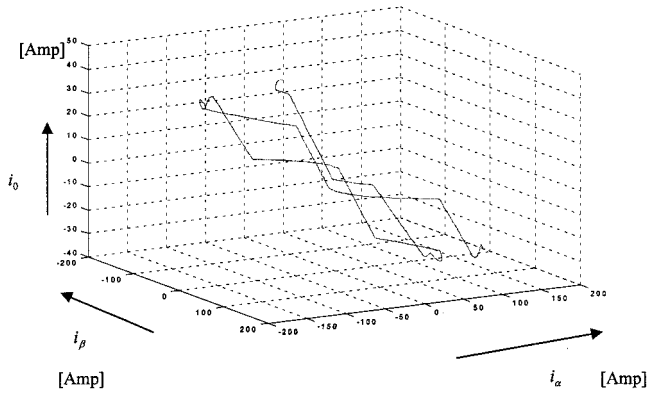

Fig. 18. Current locus before compensation in 3-D.

shows this current locus in α–β–0 frame. The performance of this three-level 3-D controller is quite acceptable with the results shown in Figs. 19 and 20. However, in this case, the switching frequency of IGBT is unfixed and it will depend on the defined limits of hysteresis value. Larger hysteresis limit will lead to have lower switching frequency and lower switching loss but with higher total harmonic distortion (higher harmonics contents). In this case, the performance is quite good when the extremely high switching frequency is employed.

C. Active Filter with Fixed Maximum Switching Frequency

In Fig. 10, there is a switch in the signals-path that the injected current from the three-level inverter into the network can be detected. In this case, that switch could determine the switching frequency of switching device (IGBT). The switching functions of S_a S_b S_c can be adjusted from one state to another and the speed of changing states will depend on the sampling rate of this switch. However, the performance of this system will be affected by the sampling rate, the inductance and resistance values of coupling transformer, voltage difference between the terminals of three-level inverter and the coupling point with the network and the values of the hysteresis limit.

The simulation is performed with the fixed maximum switching frequency. The sampling rate is 20 KHz. It means that the faster speed to change the inverter from one state to another is 1/20K s. Fig. 23 shows the load current in 3-D aspect

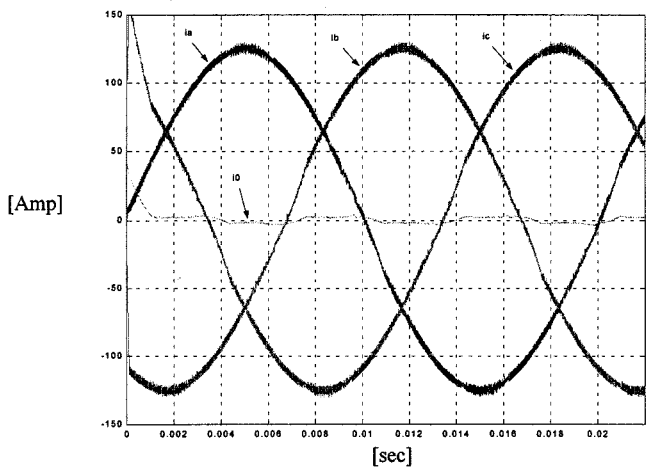

Fig. 19. Current waveforms after compensation.

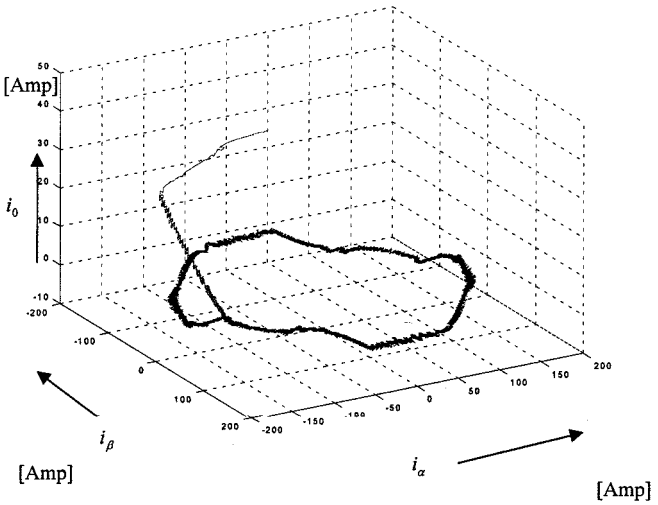

Fig. 20. Current locus after compensation in 3-D.

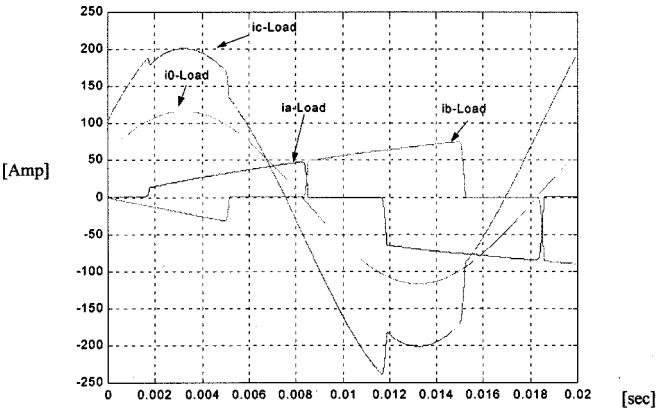

Fig. 21. Load current in time domain.

without compensation. The compensated currents are shown in Figs. 22 and 24. Comparing the Figs. 19 and 22, Fig. 19 is the compensated current with random switching frequency and switching frequency cannot be controlled except the Hysteresis

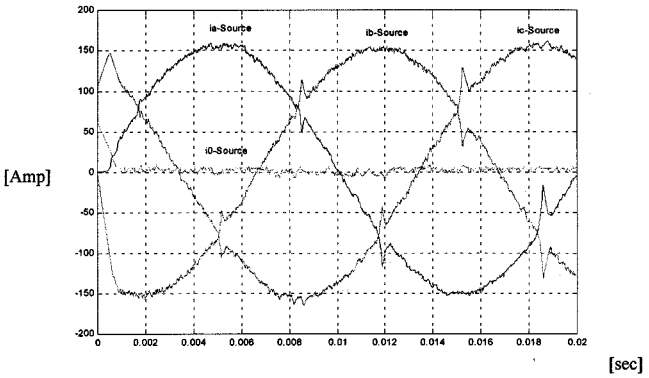

Fig. 22. Compensated current by three-level inverter.

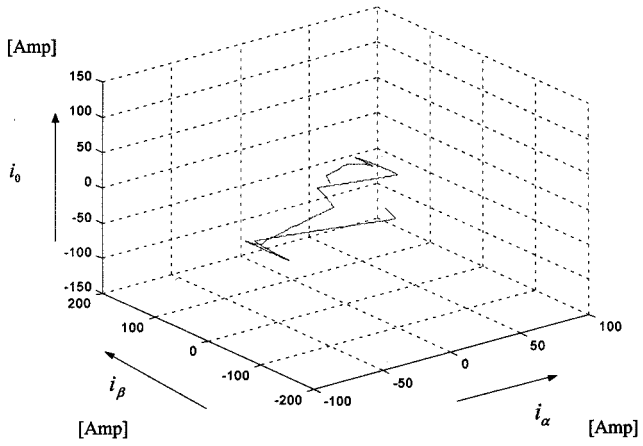

Fig. 23. Load current in 3-D.

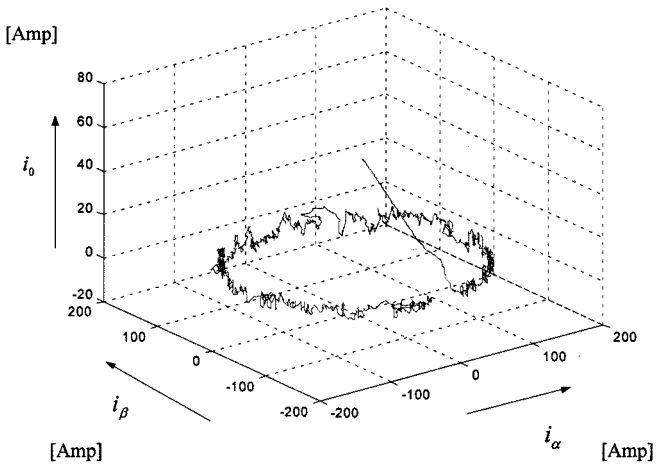

Fig. 24. Source current in 3-D by three-level inverter.

limit. However, in this case, it is not practical, as the maximum switching frequency of IGBT is limited. By the way, Fig. 22, it is obvious that the performance of this control strategy can be affected by the above-described issues at the time ≈5 ms, 8.5 ms, 11.8 ms, 15 ms and 18.2 ms. However, the performance can be improved at 5 ms, 8.5 ms, 11.8 ms, 15 ms and 18.2 ms if the size of the coupling transformer is reduced. Fig. 24 shows the compensated current in 3-D.

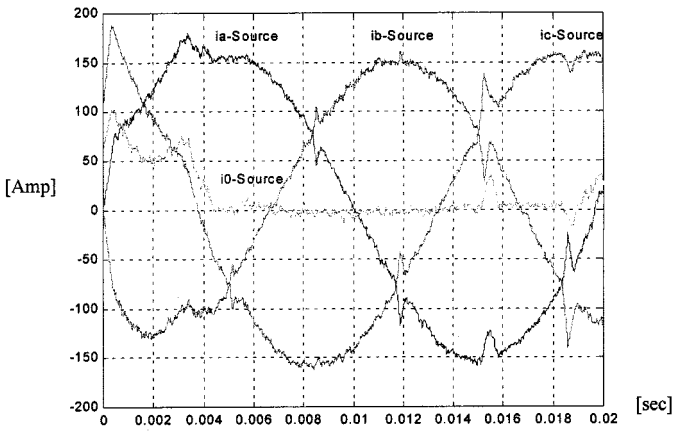

Fig. 25. Compensated current by two-level inverter.

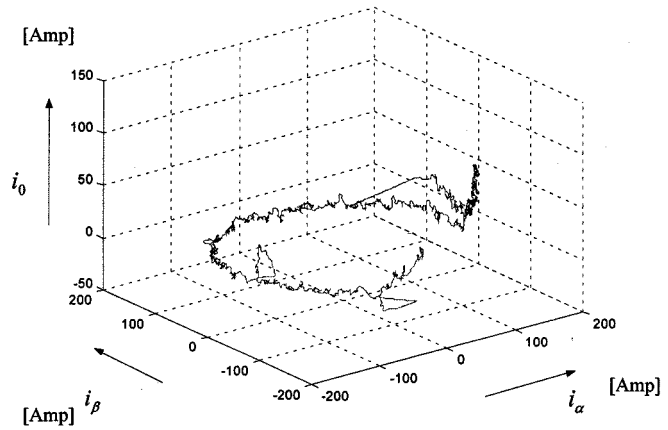

Fig. 26. Source current in 3-D by two-level inverter.

D. Comparison with Two-Level Three-Phase Four-Wired System

In a three-level system there are a total of 27 switching states. However, in two-level case, there are only eight states shown in Fig. 4 (six direction vectors and two zero vectors). But, in $\alpha\beta 0$ domain, there are a total of 27 possible situations shown in Table VIII. There are only six special vectors that will introduce error in α axis, β axis or/and 0-axis (Described in Section IV-B-2) for three-level inverter, but there are 18 special vectors in two-level system. It means that more error will be obtained and there are many possible combinations in the final table for hysteresis control technique with different error manner. By the way, three-level inverter can apply into high voltage situation. Simulation is performed for two-level system as an active filter with the same condition of three-level case by the same control strategy. Simulation results are shown in Figs. 25 and 26. From $t = 0$ s to $t = 0.4$ ms, it is obvious that i_0 is much larger than the one in three-level case. Two-level hysteresis control gives worst results than three-level one in 3-D aspect by sign cubical control method and it cannot apply into high voltage case. However, two-level 3-D PWM technique is a subset of three level one.

VI. Conclusion

The shunt-connected three-level converter in three-phase four-wired system is studied with the 3-D voltage vectors consideration. Mathematical model of trilevel converter is addressed. The novel theory of 3-D three level voltage vectors is proposed with the control of sign cubical hysteresis strategy. It shows that the validity of this 3-D three-level converter theory can be applied to compensate power quality problems in three-phase four-wired system. The performance of this system will be affected by the sampling rate, the inductance and resistance values of coupling transformer, voltage difference between the terminals of three-level inverter and the coupling point with the network and the values of the hysteresis limit. The 2-D two-level voltage vector is a subset of 3-D three-level one. The basic background of three-level converter in 3-D aspect is performed. There is more degree of freedom in choosing vectors by choosing three-level inverter than two-level one. The more special vectors mean more dedicated compensation that intends one improvement in one direction and increasing dedicated error in another direction. However, two-level 3-D PWM will give more special vectors in compensation. Two-level hysteresis control gives worst results than three-level one in 3–D aspect by sign cubical control method. In addition to that, three-level inverter can be applied in high power application.

References

[1] J. Holtz, "Pulsewidth modulation—A survey," *IEEE Trans. Ind. Electron*, vol. 99, pp. 410–420, Dec. 1992.
[2] A. Trzynadlowski, "An overview of modern PWM techniques for three-phase, voltage-controlled, voltage-source inverters," in *Proc. Conf. Rec. IEEE-ISIE'96*, Warsaw, Poland, 1996, pp. 25–39.
[3] M. P. Kazmierkowski and M. A. Dzieniakowski, "Review of current regulation techniques for three-phase PWM inverters," in *Proc. Conf. Rec. IEEE-IECON'94*, Bologna, Italy, 1994, pp. 567–575.
[4] M. P. Kazmierkowski and W. Sulkowski, "Novel space vector based current controllers for PWM-inverters," in *Proc. PESC'89*, 1989, pp. 657–664.
[5] H. Akagi, "New trends in active power filters," in *Proc. EPE'95*, vol. 1, 1995, p. 664.
[6] ——, "The state-of art of power electronics in Japan," *IEEE Trans. Power Electron*, vol. 13, pp. 345–356, Mar. 1998.
[7] L. M. Tolbert, F. Z. Peng, and T. G. Habetler, "Multilevel converters for large electric drives," *IEEE Trans. Ind. Applicat.*, vol. 35, pp. 36–44, Jan./Feb. 1999.
[8] F. Z. Peng, J. W. Mckeever, and D. J. Adams, "A power line conditioner using cascade multilevel inverters for distribution systems," *IEEE Trans. Ind. Applicat.*, vol. 34, pp. 1293–1298, Nov./Dec. 1998.
[9] P. Verdelho and G. D. Marques, "Four-wire current regulator PWM voltage converter," *IEEE Trans. Ind. Electron*, vol. 45, pp. 761–770, Oct. 1998.
[10] M.-C. Wong, C.-J. Zhan, Y. Han, Y.-D. Han, and L.-B. Zhao, "Research on trilevel shunt power quality conditioner," in *Proc. Rec. IEEE Power Eng. Soc. Winter Meeting 2000*, Jan. 23–27, 2000.

Man-Chung Wong (S'97) was born in Hong Kong in 1969. He received the B.Sc. and M.Sc. degrees in electrical and electronics engineering from the University of Macau, China, in 1993 and 1997, respectively, and is pursuing the Ph.D. degree at Tsinghua University, Beijing, China.

He was a Teaching Assistant at the University of Macau, from 1993 to 1997. Since 1998, he has been a Lecturer in the Department of Electrical and Electronics Engineering, University of Macau. His research interests are power systems, power electronics, power quality, and instrumentation.

Zheng-Yi Zhao was born in Harbin, Heilongjiang, China, in May 1975. He received the Diploma of electrical engineering in power systems and the M.S. degree in power electronics from Tsinghua University, Beijing, China, in 1998 and 2000, respectively.

His research interest is the application of power electronics technology in the power system.

Ying-Duo Han (SM'65) was born in Shenyang, Liaoning province, China, in 1938. He received the B.S. and M.S. degrees from Tsinghua University, Beijing, China, in 1962 and 1965, respectively, and the Ph.D. degree from Erlangen-Nuemberg University, Germany.

He is Professor of the Department of Electrical Engineering, Tsinghua University, and from 1986 to 1995, he was Vice-Chairman and Chairman of the E.E. Department. From 1989 to 2001, he was the Head of the Power Electronic Research Center, Tsinghua University. He is a Visiting Professor at the University of Macau, China. He is also the Vice-Chairman of the Beijing Society of Electrical Engineering and Vice-Editor of the *Electric Power System and Automation*. He has published two books and more than 100 papers. He has been engaged for more than 30 years in education and research work on electric power systems and the automation field. In recent years he has engaged in FACTS & DFACTS, intelligent control, regional stability control, new dynamic security estimation, and control based on GPS.

Dr. Han received four State-level prizes and six first and second ranked Province-level and Ministry-level prizes. He is a member of the Chinese Academy of Engineering.

Liang-Bing Zhao was born in Fuchou, China, in November 1938. He received the B.S. and M.S. degrees in engineering from the Electrical Engineering Deparment, Tsinghua University, Beijing, China, in 1962 and 1965, respectively.

He is a Professor at Tsinghua University where he is Vice-Director of the Power Electronics Engineering Research Center. He is the Head of the DC Power Source Council and the Vice-Director of the Power Source Council of China Computer Institute. His research interests are in soft switch technology, PFC, waveform control technology, custom power, and high power density switching power supplies.

Mr. Zhao is a member of the China Power Source Society.